Solution structure of human DESR1, a CSL zinc-binding protein

ARTICLE *in* PROTEINS STRUCTURE FUNCTION AND BIOINFORMATICS · APRIL 2008

Impact Factor: 2.63 · DOI: 10.1002/prot.21915 · Source: PubMed

11 AUTHORS, INCLUDING:

Jiahai Zhang
University of Science and Technology of China
86 PUBLICATIONS **1,007** CITATIONS
SEE PROFILE

W. S. Chu
University of Science and Technology of China
104 PUBLICATIONS **684** CITATIONS
SEE PROFILE

Feifei Yang
University of Science and Technology of China
9 PUBLICATIONS **12** CITATIONS
SEE PROFILE

Jihui Wu
University of Science and Technology of China
98 PUBLICATIONS **1,378** CITATIONS
SEE PROFILE

PROTEINS
STRUCTURE ■ FUNCTION ■ BIOINFORMATICS

STRUCTURE NOTE

Solution structure of human DESR1, a CSL zinc-binding protein

Fangming Wu,[1] Jiahai Zhang,[1] Jianping Sun,[1] Hongda Huang,[1] Peng Ji,[1] Wangsheng Chu,[2] Meijuan Yu,[2] Feifei Yang,[2] Ziyu Wu,[2] Jihui Wu,[1]* and Yunyu Shi[1]*

[1] National Laboratory for Physical Sciences at Microscale and School of Life Sciences, University of Science and Technology of China, Hefei, Anhui 230026, China

[2] Beijing Synchrotron Radiation Facility, Institute of High Energy Physics, Chinese Academy of Sciences, Beijing 100049, China

Key words: DPH3; DelGIP1; NMR spectroscopy; EXAFS; zinc finger.

INTRODUCTION

Mammalian DESR1 was first discovered in a mutant Chinese hamster ovary cell line that is completely resistant to several different bacterial ADP-ribosylating toxins. The gene that encodes DESR1 is termed diphtheria toxin (DT) and Pseudomonas exotoxin A (ETA) sensitivity required gene 1 (*DESR1*).[1]

DESR1, also designated Dph3, is required for the first step in the posttranslational modification of translation elongation factor 2 (eEF-2) at H715 (H699 in yeast) that yields diphthamide, the target site for ADP ribosylation by DT and ETA.[1] ADP-ribosylation of eEF-2 inhibits the protein synthetic process required to maintain cell viability.[2] Recent investigation had attested to the physiological importance of Dph3 in mouse embryonic and placental development.[3]

In yeast, *DESR1/Dph3* was independently identified as *KTI11* (*Kluyveromyces lactis* toxin insensitive gene 11), which is one of the factors required for conferring sensitivity of *S. cerevisiae* to *K. lactis* zymocin[4,5] and involved in modulating the functions of the Elongator complex.[6] Recently, KTI11 was shown to be required for posttranscriptional modification of tRNA at the wobble position of the anticodon.[7]

Human DESR1 (hDESR1) was also identified as DelGEF interacting protein 1 (DelGIP1), and was reported to negatively regulate the interaction between DelGEF and Sec5, thereby negatively regulating the extracellular secretion of proteoglycans by HeLa cells.[8]

Human DESR1 and KTI11 from yeast belong to a highly conserved CSL zinc finger-containing protein family in eukaryotes (Pfam: PF05207). The mouse DESR1/Dph3 protein is also classified in this Pfam (97 proteins; Pfam 22.0).

Previously, we determined the solution structure of KTI11, which shares 37% identity with hDESR1.[9] In this article, we elucidate the solution structure of hDESR1.

MATERIALS AND METHODS

The gene of DESR1 was PCR amplified from Human Brain cDNA Library (BD Biosciences) and cloned into the NdeI/XhoI sites of pET-22b(+) vector (Novagen). The triple codon of the last residue (C82) was deleted in the 3′-primer to avoid any unexpected disulfide bond. PCR site-directed mutagenesis was carried out to replace C66 with serine for the same purpose.

The recombinant protein was expressed in *E. coli* BL21(DE3)Gold (Stratagene) cells in M9 media supple-

The Supplementary Material referred to in this article can be found online at http://www.interscience.wiley.com/jpages/0887-3585/suppmat/.

Grant sponsor: Chinese National Fundamental Research Project; Grant numbers: 2002CB713806, 2006CB806507, 2006CB910201; Grant sponsor: Chinese National Natural Science Foundation; Grant numbers: 30121001, 30570361, 30670426; Grant sponsor: National Outstanding Youth Fund; Grant number: 10125523; Grant sponsor: Key Important Project of the National Natural Science Foundation of China; Grant numbers: 10490190, 10490191, 10490193.

*Correspondence to: Jihui Wu, School of Life Sciences, University of Science and Technology of China, Hefei, Anhui 230026, China. E-mail: wujihui@ustc.edu.cn or Yunyu Shi, School of Life Sciences, University of Science and Technology of China, Hefei, Anhui 230026, China. E-mail: yyshi@ustc.edu.cn

Received 26 September 2007; Revised 1 November 2007; Accepted 8 November 2007

Published online 23 January 2008 in Wiley InterScience (www.interscience.wiley.com). DOI: 10.1002/prot.21915

mented with 0.1 m*M* $ZnSO_4$, and induced with 0.5 m*M* IPTG at 16°C for 20 h. The isotopically enriched protein was prepared using ^{15}N-NH_4Cl and ^{13}C-D-glucose as the sole nitrogen and carbon sources. The protein was purified using Ni-NTA Superflow column (Qiagen) and then HiLoad 16/60 Superdex 75 column (Amersham). All the samples for NMR contained 20 m*M* Tris-HCl buffer (pH 7.0), 50 m*M* NaCl and 14 m*M* β-ME in a 90% H_2O/10% D_2O mixture or in 99.96% D_2O.

The EXAFS measurements were conducted in "fluorescence yield" mode using a Si(111) double crystal monochromator, at the X-ray absorption station (beamline 1W1B) of Beijing Synchrotron Radiation Facility (BSRF). A detuning of 30% was performed by the monochromator to suppress the unwanted harmonics. The incident beam intensity was monitored by an ionization chamber flowed with 25% Ar/75% N_2, and the fluorescence signal was recorded by a Lytle detector flowed with 100% Ar.

2D ^{1}H, ^{15}N-HSQC, 3D HNCO, HN(CA)CO, CBCANH, CBCA(CO)NH, C(CO)NH-TOCSY, H(CCO)NH-TOCSY, HBHA(CBCACO)NH, HCCH-TOCSY, HCCH-COSY, 3D ^{15}N-separated NOESY (mixing time 100 ms) and 3D ^{13}C-separated NOESY (mixing time 130 ms) spectra were collected using Bruker DMX600 spectrometer. NMR data were processed using NMRPipe[10] and analyzed with Sparky.

NMR distance restraints were obtained from the NOESY spectra. Backbone dihedral angle restraints were derived by the analysis of $^{13}C^{\alpha}$, $^{13}C^{\beta}$, $^{13}C'$, ^{15}N, $^1H^{\alpha}$ chemical shifts using TALOS.[11] Hydrogen bond restraints were determined based on slow exchanging amide protons identified by recording ^{1}H, ^{15}N HSQC after dissolving the lyophilized ^{15}N-labeled protein sample in 99.96% D_2O. Zinc coordination restraints were derived from EXAFS experiments and data processing.

The structures were calculated using CNS v1.1.[12] The preliminary structures were calculated only with NMR-derived restraints, and the best structure was used as the model for EXAFS analysis. Then the zinc coordination restraints were included in the later stage of structure calculation. The quality of structures was assessed using PROCHECK-NMR[13] and MOLMOL.[14]

The chemical shifts for hDESR1 have been deposited in BioMagResBank (accession code: 15377) and coordinates for the 20 structures have been deposited into RCSB PDB with the list of restraints used for the structure calculation (PDB entry 2JR7).

RESULTS AND DISCUSSION

Bioinformatics suggest that *hDESR1* encodes a CSL zinc finger (Pfam PF05207). The presence of a single zinc ion was confirmed by atomic absorption spectroscopy (data not shown). The four conserved cysteines (C26, C28, C48, and C51) are proposed to be potential zinc-binding ligands.

Table I
Structural Statistics for the Final 20 Conformers of Human DESR1[a]

Structural restraints	
Intraresidue	279
Sequential	453
Medium-range ($2 \leq \|i-j\| \leq 4$)	239
Long-range ($\|i-j\| \geq 5$)	566
Dihedral restraints	60
Hydrogen bond restraints	20
Zinc coordination restraints	10
Total	1627
Statistics for 20 structures	
RMSD from experimental restraints	
Distance	0.0067 ± 0.0002
Dihedral	0.0797 ± 0.0110
RMSD from idealized covalent geometry	
Bond lengths (Å)	0.0008 ± 0.00002
Bond angles (deg)	0.2665 ± 0.0011
Improper angles (deg)	0.0973 ± 0.0015
Lennard-Jones potential energy (kcal/mol)	−226.9 ± 8.58
Coordinate precision	
RMSD to the mean (Å)	backbone/heavy
Residues 4-66	0.366/0.757
Residues in secondary structure elements	0.204/0.679
Ramachandran plot statistics (%)[b]	
Most favored regions	71.9
Additional allowed regions	25.9
Generously allowed regions	1.2
Disallowed regions	0.9

[a]None of the structures exhibits distance violations greater than 0.2 Å or dihedral angle violations greater than 5°.
[b]Determined using the program PROCHECK-NMR.[13]

EXAFS spectroscopy was used to define the local structure around the zinc ion. Figure S1(A) shows the experimental EXAFS spectrum and the calculated spectrum by FEFF8[15] based on the structural information of NMR. They are quite similar, thus, it can be concluded that the zinc ion is coordinated by the four sulfur atoms from the four conserved cysteines. In order to get further local structure information, the EXAFS spectrum at Zn K-edge of hDESR1 was fitted by WinXAS v3.1,[16] as shown in Figure S1(B). We used the four sulfur atoms to fit the spectrum. The EXAFS analysis gave the coordination number of the first shell around zinc ion 3.8 ± 0.2, the Zn-S bond length 2.35 ± 0.01 Å, and Debye-Waller factor 0.009 ± 0.002 $Å^2$.

About 94% of backbone resonances (C^{α}, CO, NH, and N) and 84% of side chain resonances (^{1}H) were assigned by taking no account of the 6 His-tag residues. The structure of hDESR1 has been determined on the basis of 1627 restraints, which contain 1537 interproton distance restraints, 60 dihedral angle restraints, 20 hydrogen bonds restraints, and 10 zinc coordination restraints. The 20 lowest energy structures were selected out of 200 accepted structures, and the statistics about the quality and precision of them are summarized in Table I. The backbone superimposition of the final 20 conformers and

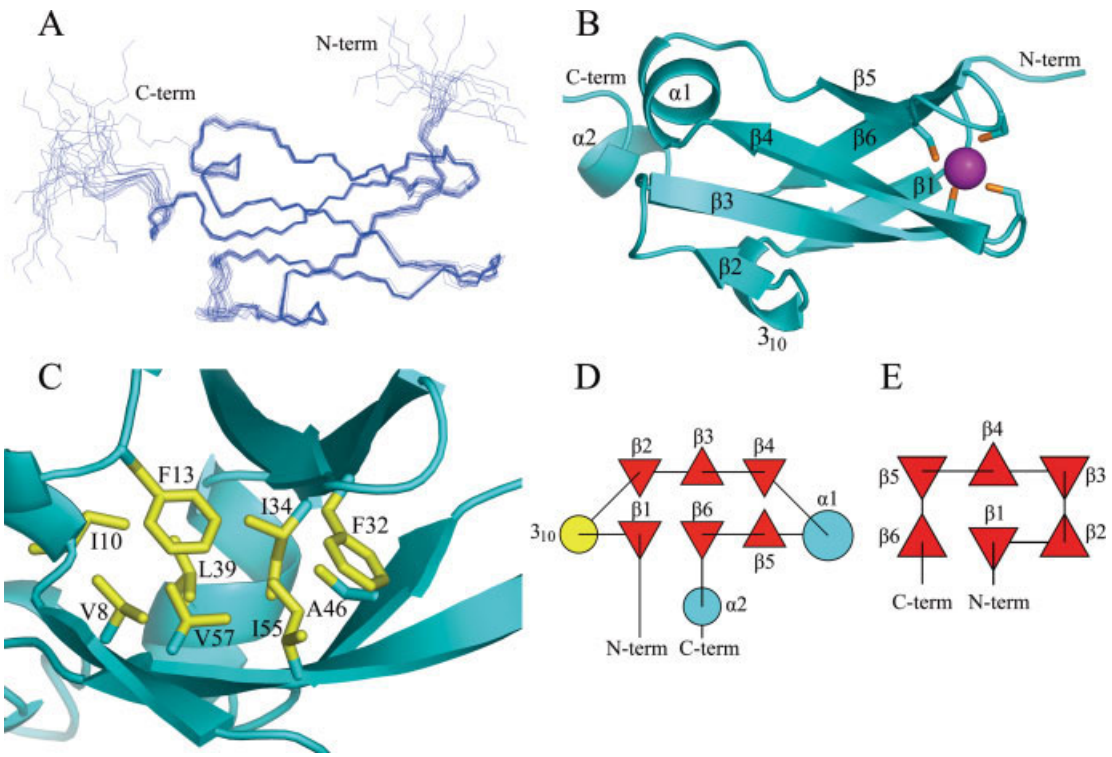

Figure 1

*(**A**) The backbone superposition of the final 20 conformers. (**B**) The cartoon representation of the structure of hDESR1. (The unstructured C-terminal residues following P71 are excluded.) Orange sticks, zinc-binding cysteines; magenta sphere, zinc ion. (**C**) The hydrophobic core of hDESR1. The topology diagrams of hDESR1 (**D**) and S27e (**E**). [Color figure can be viewed in the online issue, which is available at www.interscience.wiley.com.]*

the representative structure are presented in Figure 1(A,B).

The structure consists of six β-strands, a 3_{10} helix, and two α helices [Fig. 1(B)]. The six β-strands form two three-stranded β-sheets with topology β1(↑), β6(↑), β5(↓), and β2(↑), β3(↓), β4(↑). The 3_{10} helix between β1 and β2 and α1 between β4 and β5 separate the two β-sheets. The structural topology was visualized for hDESR1 using TOPS[17] in Figure 1(D).

The four cysteines that coordinate the zinc ion are located in the knuckles protruding from the two hairpins between β3 and β4 and between β5 and β6. Zinc coordination by the four cysteine residues was also confirmed by chemical shift data. The chemical shifts of their C^{β} atoms were found to be between 29.5 and 31.5 ppm, consistent with the cysteines in reduced state[18] and the sulfur groups coordinating zinc ions. Furthermore, C48 has a C^{α}/C^{β} chemical shift vector residing within the >50% Zn-ligated probability region, while C26 resides just outside of but very close to this region, and the two remaining cysteines (C28 and C51) reside in the >90% Zn-ligated probability region, according to Kornhaber's hierarchical logits model.[19]

A hydrophobic core is formed in hDESR1 by the interactions between the side chains of the conserved hydrophobic residues such as V8, I10, F13, F32, I34, L39, A46, I55, and V57 [Fig. 1(C)].

Altogether, the zinc ion, the hydrophobic core, and the three helices are spatially arranged in a line and lie in the interval between the two β-sheets to form a sandwich that contributes to the stability of the entire structure.

The theoretical pI of 3.94 indicates that hDESR1 is an acidic protein. There are 19 negatively charged residues and 13 out of them are highly conserved (D6, 12, 16, 18, 30, 38, 60, 62; E7, 9, 11, 37, 43). The electrostatic potential surface of hDESR1 shows a negatively charged surface that covers the majority of the protein (Fig. S2), which suggests that hDESR1 interacts with positively charged molecules.

The sequence alignment of hDESR1 and its homologues illustrates the high conservation between species especially in the region encoded by exon 1 and 2. The region corresponding to exon 3, however, is divergent [Fig. 2(A)]. In addition, the two loops, which include the four zinc coordinated cysteines, are more conserved than any secondary structure regions. This fact implies that

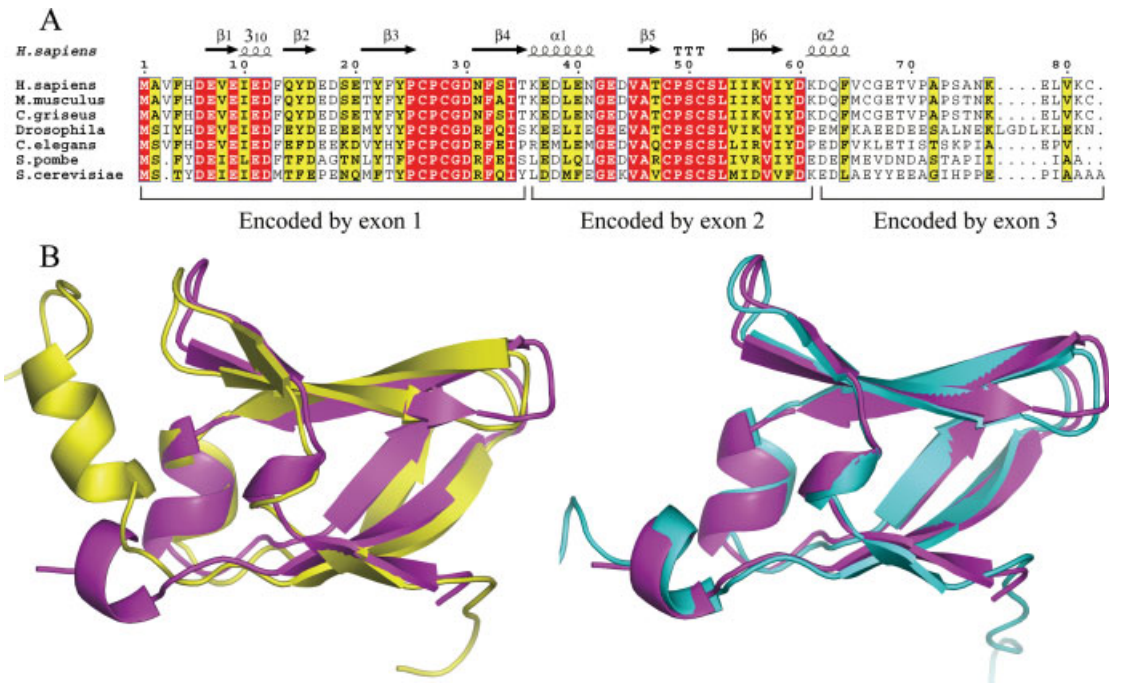

Figure 2

*(**A**) Multiple sequence alignment of hDESR1 and its homologues. The alignments were generated by ClustalW[20] and decorated using ESPript.[21] The secondary structure of hDESR1 is displayed over the alignment. All conserved residues are highlighted. The three fragments encoded by the three exons are marked. (**B**) Structural comparison of hDESR1 (magenta) with KTI11 (1YOP, yellow) and mDESR1 (1WGE, cyan).*

these two zinc binding loops are the most important parts of them and that the zinc ion plays an essential role in maintaining the stability of the whole structure.

Proteins with similar 3D structures were searched against the PDB using Dali[22] and SSM.[23] Dali compares a single input structure against a representative set from the PDB. No similar structures were detected when hDESR1 was used as the bait. Furthermore, SSM search was carried out against the entire PDB. The core domain of hDESR1 (residue 4–66) was used as the query structure. In the results, three of them showed obvious similarity with hDESR1. The first hit with highest Z (8.6) score and lowest RMSD (0.81 Å) is the solution structure of mouse DESR1 (1WGE, DOI 10.2210/pdb1wge/pdb, Yokoyama *et al.*, unpublished results) which shares 96% identity with hDESR1. The other two hits, 1YWS and 1YOP, are both the solution structure of KTI11, determined by Arrowsmith's group (DOI 10.2210/pdb1yws/pdb, unpublished results) and Sun *et al.*,[9] respectively. The structure of hDESR1 was compared with KTI11 and mDESR1 (mouse DESR1) by using DaliLite.[24] Figure 2(B) shows the superposition with the most residues aligned. These structures exhibit great similarity to each other. The most obvious difference between these three proteins is that KTI11 has a long α helix from K61 to E70 while mouse/human DESR1 only possess a short one that terminates at M/V65. This difference occurs within hDESR1 residues 61–70 which is encoded by exon 3, consistent with the loss of conservation and function of this region. The function of DESR1 is mainly determined by the amino-terminal portion of the protein; the first 61 residues of hDESR1 are sufficient to complement the *KTI11* mutation in *S. cerevisiae*.[1]

Another zinc finger protein (the 30S ribosomal protein S27e of *Archaeoglobus fulgidis*[25]), has a similar protein structure topology with hDESR1. The topology diagram of S27e (PDB entry 1QXF) is shown in Figure 1(E) and compared with that of hDESR1. These two TOPS cartoons overlap each other very well when the N-terminus of DESR1 is superimposed with the C-terminus of S27e and vice versa. The arrangement of strands is almost the same except the direction of the left strand in the bottom sheet.

The structure of hDESR1 should be classified into the Cys_4 ribbon family and the zinc ribbon fold group according to the classification of Leon and Roth[26] and the definitions of zinc fingers database,[27] respectively.

The structure of KTI11 (1YOP, 1YWS) and mDESR1 (1WGE) has not yet been classified in CATH.[28] DESR1 could be assigned to the rubredoxin-like fold of the small proteins class in the SCOP[29] classification. These proteins comprise a metal (zinc or iron)-bound fold, contain

two $CX_{(n)}C$ motifs (in most cases $n = 2$) and the current SCOP classification (1.71 release) encompasses 14 superfamilies. FastSCOP[30] was employed to recognize the evolutionary classifications of DESR1 and KTI11, but they could not be assigned. Thus, the structures of DESR1 and KTI11 may be examples of a novel SCOP classification. On the basis of the above facts, it is believed that hDESR1 and its homologues belong to a new superfamily.

In summary, we solved the structure of hDESR1 providing helpful information for further functional analysis. Our further investigations will focus on the structural basis of protein–protein interactions between hDESR1 and its partners.

ACKNOWLEDGMENT

We thank Dr. T. D. Kneller for providing Sparky and Dr. L. D. Warren for providing PyMOL. We also gratefully thank Dr. A. Kwan for kind help in structural calculation and Dr. C. Rasmussen for critical reading of the manuscript.

REFERENCES

1. Liu S, Leppla SH. Retroviral insertional mutagenesis identifies a small protein required for synthesis of diphthamide, the target of bacterial ADP-ribosylating toxins. Mol Cell 2003;12:603–613.
2. Collier RJ. Understanding the mode of action of diphtheria toxin: a perspective on progress during the 20th century. Toxicon 2001;39: 1793–1803.
3. Liu S, Wiggins JF, Sreenath T, Kulkarni AB, Ward JM, Leppla SH. Dph3, a small protein required for diphthamide biosynthesis, is essential in mouse development. Mol Cell Biol 2006;26:3835–3841.
4. Butler AR, White JH, Folawiyo Y, Edlin A, Gardiner D, Stark MJ. Two *Saccharomyces cerevisiae* genes which control sensitivity to G1 arrest induced by *Kluyveromyces lactis* toxin. Mol Cell Biol 1994;14: 6306–6316.
5. Fichtner L, Schaffrath R. KTI11 and KTI13, *Saccharomyces cerevisiae* genes controlling sensitivity to G1 arrest induced by *Kluyveromyces lactis* zymocin. Mol Microbiol 2002;44:865–875.
6. Fichtner L, Jablonowski D, Schierhorn A, Kitamoto HK, Stark MJ, Schaffrath R. Elongator's toxin-target (TOT) function is nuclear localization sequence dependent and suppressed by post-translational modification. Mol Microbiol 2003;49:1297–1307.
7. Huang B, Johansson MJ, Bystrom AS. An early step in wobble uridine tRNA modification requires the Elongator complex. RNA 2005;11:424–436.
8. Sjolinder M, Uhlmann J, Ponstingl H. Characterisation of an evolutionary conserved protein interacting with the putative guanine nucleotide exchange factor DelGEF and modulating secretion. Exp Cell Res 2004;294:68–76.
9. Sun J, Zhang J, Wu F, Xu C, Li S, Zhao W, Wu Z, Wu J, Zhou CZ, Shi Y. Solution structure of Kti11p from *Saccharomyces cerevisiae* reveals a novel zinc-binding module. Biochemistry 2005;44:8801–8809.
10. Delaglio F, Grzesiek S, Vuister GW, Zhu G, Pfeifer J, Bax A. NMRPipe: a multidimensional spectral processing system based on UNIX pipes. J Biomol NMR 1995;6:277–293.
11. Cornilescu G, Delaglio F, Bax A. Protein backbone angle restraints from searching a database for chemical shift and sequence homology. J Biomol NMR 1999;13:289–302.
12. Brunger AT, Adams PD, Clore GM, DeLano WL, Gros P, Grosse-Kunstleve RW, Jiang JS, Kuszewski J, Nilges M, Pannu NS, Read RJ, Rice LM, Simonson T, Warren GL. Crystallography & NMR system: a new software suite for macromolecular structure determination. Acta Crystallogr Sect D 1998;54:905–921.
13. Laskowski RA, Rullmannn JA, MacArthur MW, Kaptein R, Thornton JM. AQUA and PROCHECK-NMR: programs for checking the quality of protein structures solved by NMR. J Biomol NMR 1996;8:477–486.
14. Koradi R, Billeter M, Wuthrich K. MOLMOL: a program for display and analysis of macromolecular structures. J Mol Graph 1996;14:51–55, 29–32.
15. Ankudinov AL, Ravel B, Rehr JJ, Conradson SD. Real-space multiple-scattering calculation and interpretation of X-ray-absorption near-edge structure. Phys Rev B 1998;58:7565.
16. Ressler T, Brock SL, Wong J, Suib SL. Multiple-scattering EXAFS analysis of tetraalkylammonium manganese oxide colloids. J Phys Chem B 1999;103:6407–6420.
17. Michalopoulos I, Torrance GM, Gilbert DR, Westhead DR. TOPS: an enhanced database of protein structural topology. Nucleic Acids Res 2004;32:D251–D254.
18. Atreya HS, Sahu SC, Chary KV, Govil G. A tracked approach for automated NMR assignments in proteins (TATAPRO). J Biomol NMR 2000;17:125–136.
19. Kornhaber GJ, Snyder D, Moseley HN, Montelione GT. Identification of zinc-ligated cysteine residues based on 13Calpha and 13Cbeta chemical shift data. J Biomol NMR 2006;34:259–269.
20. Higgins DG, Sharp PM. CLUSTAL: a package for performing multiple sequence alignment on a microcomputer. Gene 1988;73:237–244.
21. Gouet P, Courcelle E, Stuart DI, Metoz F. ESPript: analysis of multiple sequence alignments in PostScript. Bioinformatics 1999;15:305–308.
22. Holm L, Sander C. Protein structure comparison by alignment of distance matrices. J Mol Biol 1993;233:123–138.
23. Krissinel E, Henrick K. Secondary-structure matching (SSM), a new tool for fast protein structure alignment in three dimensions. Acta Crystallogr Sect D 2004;60:2256–2268.
24. Holm L, Park J. DaliLite workbench for protein structure comparison. Bioinformatics 2000;16:566–567.
25. Herve du Penhoat C, Atreya HS, Shen Y, Liu G, Acton TB, Xiao R, Li Z, Murray D, Montelione GT, Szyperski T. The NMR solution structure of the 30S ribosomal protein S27e encoded in gene RS27_ARCFU of *Archaeoglobus fulgidis* reveals a novel protein fold. Protein Sci 2004;13:1407–1416.
26. Leon O, Roth M. Zinc fingers: DNA binding and protein-protein interactions. Biol Res 2000;33:21–30.
27. Krishna SS, Majumdar I, Grishin NV. Structural classification of zinc fingers: survey and summary. Nucleic Acids Res 2003;31:532–550.
28. Orengo CA, Michie AD, Jones S, Jones DT, Swindells MB, Thornton JM. CATH—a hierarchic classification of protein domain structures. Structure 1997;5:1093–1108.
29. Lo Conte L, Ailey B, Hubbard TJ, Brenner SE, Murzin AG, Chothia C. SCOP: a structural classification of proteins database. Nucleic Acids Res 2000;28:257–259.
30. Tung CH, Yang JM. fastSCOP: a fast web server for recognizing protein structural domains and SCOP superfamilies. Nucleic Acids Res 2007;35:W438–W443.